Thin Solid Films 553 (2014) 93–97

Contents lists available at ScienceDirect

Thin Solid Films

journal homepage: www.elsevier.com/locate/tsf

Structural and electrical properties in tungsten/tungsten oxide multilayers

Arnaud Cacucci [a], Valérie Potin [a,*], Luc Imhoff [a], Nicolas Martin [b]

[a] Laboratoire Interdisciplinaire Carnot de Bourgogne, UMR 6303 CNRS-Université de Bourgogne, 9 Avenue Alain Savary, BP47870, F-21078 DIJON Cedex, France
[b] Institut FEMTO-ST, UMR 6174 CNRS, Université de Franche-Comté, ENSMM, UTBM, 32 Avenue de l'observatoire, F-25044, BESANCON Cedex, France

ARTICLE INFO

Available online 28 October 2013

Keywords:
Tungsten oxide
Thin films
Periodic multilayers
Reactive sputtering
Gas pulsing
Electrical properties

ABSTRACT

Tungsten and tungsten oxide periodic nanometric multilayers have been deposited by DC reactive sputtering using the reactive gas pulsing process. Different pulsing periods have been used for each deposition to produce metal-oxide periodic alternations ranging from 3.3 to 71.5 nm. The morphology, crystallinity and chemical composition of these films have been investigated by transmission electron microscopy and energy-dispersive X-ray spectroscopy techniques. The produced multilayers exhibited an amorphous structure and the composition stability of WO_3 sub-layers has been pointed out. Moreover, electrical properties have also been studied by the van der Pauw technique. It revealed a clear stability of resistivity versus temperature for almost all samples and an influence of the multilayered structure on the resistivity behavior.

1. Introduction

Tungsten oxide compounds have a great technological interest, particularly because of their optical and electrical performances [1–4]. Many investigations are focused on tungsten oxide thin films because of their applications in electrochromic devices and gas sensors [5–9]. These films can be changed in a reversible and persistent way under the influence of an applied voltage [10]. Because of such technological attraction, tungsten oxide thin films have been produced with a large variety of deposition methods including anodization, thermal oxidation, ion-assisted deposition, chemical and physical vapor deposition [11–15]. The WO_x films prepared by these different techniques showed widely dispersed properties depending on the process parameters, temperature growth, post-annealing conditions, etc. Tungsten oxides are also known for their sensitivity for gas sensor applications [16–18]. However, their semi-conducting behavior as a function of temperature [19] requires electronic and/or thermal addition devices to determine and/or stabilize the material resistivity at each temperature for an accurate detection of gaseous species. Therefore, the purpose is to combine the linear resistivity versus temperature of the pure metal (W) with the WO_x behavior to create a sensitive material without resistivity variation versus temperature for a basic gas sensor application. Previous works have shown that electrical resistivity can be modulated and controlled by structuring metal and semi-conductor in nanometric and periodic multilayered systems [20].

The present work is devoted to the synthesis of tungsten-based metal/oxide multilayered films by DC reactive magnetron sputtering with a controlled pulsing flow rate of the reactive gas. The O_2 flow rate is periodically changed versus time according to a rectangular wave function. Different pulsing periods, O_2 introduction and stopping times t_{on} and t_{off}, respectively, are used in order to compare the influence of the RGPP (Reactive Gas Pulsing Process) growth parameters on the nanometric structure of tungsten oxide multilayered systems. The latter technique was used for its ability to produce tunable compositions [21–27] of metallic nitrides, oxides, carbides, oxynitrides, carbonitrides … and also to perform nanometric and periodic multilayers with paired metal/semi-conductor materials [20,28–30].

The purpose of this paper is to show how structuration in periodic thin multilayers can influence the electrical properties of WO_x films. The role of the total period thickness Λ and the χ parameter defined as the ratio $\lambda_{met}/\lambda_{ox}$ (where λ_{met} is the thickness of the metal sub-layer and λ_{ox} that of the oxide one) on the properties of the films is principally investigated.

2. Experimental details

Thin films were simultaneously deposited onto (100) silicon wafers and glass substrates at room temperature by DC reactive magnetron sputtering from a tungsten metallic target (purity 99.6 at.% and 51 mm diameter) in an $Ar + O_2$ gas mixture. The target was sputtered with a constant current density $J = 50\,A\,m^{-2}$. The distance between the target and the substrate was fixed at 65 mm. The gas flow rates were controlled by a homemade system [31]. Before introducing the reactive gas, the base pressure in the chamber was about 2.10^{-5} Pa. All depositions were carried out with an argon flow rate of 2.4 sccm and a constant pumping speed of $13\,L\,s^{-1}$, which produced an argon partial pressure of 0.28 Pa. The oxygen mass flow rate was periodically controlled versus time according to a rectangular signal by the reactive gas pulsing

* Corresponding author. Tel.: +33 3 80 39 59 23; fax: +33 3 80 39 50 69.
E-mail address: valerie.potin@u-bourgogne.fr (V. Potin).

0040-6090/$ – see front matter © 2013 Elsevier B.V. All rights reserved.
http://dx.doi.org/10.1016/j.tsf.2013.10.098

process [32]. The pulsing period T of the oxygen flow rate was changed from 12 to 500 s to produce fifteen different periodic metal/oxide alternations (W_{pure} and W_1 to W_{14} samples). The maximum O_2 flow rate was fixed at 2 sccm during the t_{on} injection time. Otherwise it was completely stopped (no oxygen injection) during the t_{off} time. The expected tungsten/tungsten oxide period thickness Λ is in-between 5 to 100 nm, with $\Lambda = \lambda_{met} + \lambda_{ox}$, where λ_{met} and λ_{ox} are the thicknesses of the metal and oxide sub-layers, respectively. As a result, the duty cycle α defined as the ratio t_{on}/T takes values from 14 to 40% of T in order to tune the $\lambda_{ox}/\lambda_{met}$ ratio. Moreover, the deposition procedure always started with the O-rich layer and finished with the W-rich one.

The crystalline structure was analyzed by X-ray diffraction (XRD) in θ/2θ configuration using a monochromatized Co Kα radiation. Scans were performed with a step of 0.02° per 0.2 s and a 2θ angle ranging from 20 to 80°. Then, for all samples the local structure was studied by high resolution transmission electron microscopy (HRTEM) to check the thickness, interface and local order in each sub-layer. The chemical composition was determined by energy-dispersive X-ray (EDX) spectroscopy in scanning mode (STEM) implemented in a TEM JEOL 2100 FEG with a scanning probe size varying from 0.5 to 2 nm. Moreover, DC electrical resistivity ρ of the films deposited on glass substrates was performed versus temperature from 25 to 200 °C with a homemade system based on the van der Pauw method.

3. Results and discussion

3.1. XRD and HRTEM study

Fig. 1 shows the XRD patterns obtained from a series of tungsten oxide multilayers deposited on a silicon substrate. These samples are characterized by the variation of the multilayered period thickness Λ from 3.3 to 71.5 nm. The broad diffraction bands reveal the poorly crystallized structure of the films as compared to the silicon bulk signal. Indeed, by taking into account the thickness probed by X-ray (about 450 nm), the amorphous characteristic of this material is pointed out by the relative peaks intensity between the tungsten based phases and the (001) Si single crystal substrate. Moreover, there is no crystallization for multilayers with a total period $\Lambda < 10$ nm. Then, this diffractogram clearly points out the increase of crystal occurrence with the total period Λ. An intense peak appears at $2\theta = 46.8°$ for $17 < \Lambda < 44$ nm, corresponding to three different tungsten compounds: β-W, β-W_3O and monoclinic WO_3. For $\Lambda > 45$ nm, XRD patterns reveal a second peak at $2\theta = 41.7°$ which also corresponds to the three compounds previously reported. The occurrence of the WO_3 monoclinic phase can actually be excluded as WO_3 peaks intensity is very low for both 2θ values. Moreover, many other characteristic peaks of this WO_3 phase should have been observed in this XRD diffractogram. Indeed, Fig. 1 shows that the pure metal layer crystallizes according to the β-W phase and that the tungsten-based multilayers correspond to β-W and/or β-W_3O phases. The third peak at $2\theta = 51.5°$ (only for the pure metal sample) can be explained by a lower amount of metallic compounds (β-W or β-W_3O) in multilayered systems than in the pure metal layer. So, it is quite ambiguous to distinguish if β-W or β-W_3O or a phase mixture can be assigned from XRD patterns. In addition, Petroff et al. [33] showed that β-W is an A3B compound, which can be stabilized by small amounts of oxygen. A more detailed study about this film structure is required in order to better understand which phases appear even if these multilayered systems are mostly amorphous.

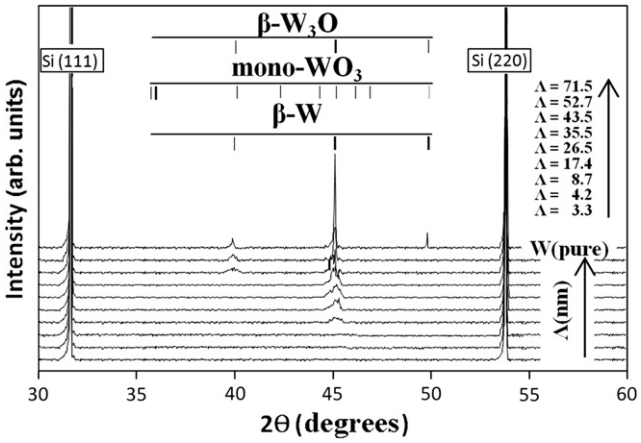

Fig. 1. XRD diffractograms of pure W and samples characterized by Λ ranging from 3.3 to 71.5 nm. References of β-W, β-W_3O and WO_3 are from ICDD 00-047-1319, 01-073-2526 and 01-072-0677, respectively.

The cross-sectional observations by TEM reveal distinct alternations of tungsten (dark bands) and tungsten oxide (bright bands) sub-layers for all samples. Clear interfaces between sub-layers can be observed (Fig. 2.a). TEM allows nanometric measurements (±1 nm) for total thickness (t_{tot}) and sub-nanometric ones (±0.2 nm) for periods and sub-layer thicknesses (Λ and λ, respectively). The period thickness Λ is included in-between 3.3 and 71.5 nm, with t_{tot} ranging from 300 to 560 nm (Fig. 2.b). Similarly, metallic and oxide sub-layer thicknesses λ_{met} and λ_{ox} are measured for all samples as reported in Table 1. TEM micrographs systematically indicate that the interface between the silicon substrate and the grown multilayers is flat and regular. As expected, the thickness of the native SiO_x layer is close to 3.0 nm. These TEM observations show that the dimension of the period stacks (two sub-layers) is accurately controlled during the growth and remains constant from the substrate to the surface. DC reactive sputtering with the RGPP technique produced sub-layer thicknesses lower than 2 nm as it can be observed in Fig. 2.b. Indeed, this technique allows obtaining λ_{met} included between 1.3 nm and 41 nm, and λ_{ox} between 2 nm and 30.5 nm, respectively.

Energy-dispersive X-ray spectroscopy analyses were performed in STEM mode in order to determine the sub-layers elemental chemical composition. Four measurements were systematically performed on the same sub-layer and two other sub-layers were also analyzed. The average value is reported in Table 1 and the accuracy is calculated from the standard deviation. In the O-rich sub-layers, the amount of W and O is 25 at.% and 75 at.%, respectively, with a variation of less than 4% for all samples. This reveals an oxide phase of composition close to WO_3. For the W-rich sub-layers, the EDX measurements show that this sub-layer is mainly composed by tungsten with 95 at.% of W and 5 at.% of O. The composition of the metal sub-layer is higher than 75 at.% for $\lambda_{met} > 10$ nm. So the occurrence of two phases can be possible with some inclusions of tungsten oxide W_3O in the pure metallic sub-layer. For metallic periods thinner than 10 nm, the composition appears to be close to a WO compound. This variation of W amount in the metal sub-layer can be explained by two reasons linked to the state of the W target surface during sputtering. The first one is due to an oxidation of the target surface. Actually, during the t_{on} time, the surface of the metallic target becomes fully oxidized after a few seconds. As a result, the target oxidation state is different for all samples because of the different oxygen time injection (t_{on}). Secondly, the target erosion induced by the magnetron effect can also explain the different amounts of W in each sample.

HRTEM images and diffraction patterns analyses allow the observation of some eventual crystalline phases. By comparing experimental and simulated (JEMS software [34]) patterns, the determination and identification of the crystal structure are accurately done. HRTEM pictures highlight that the W-rich sub-layers are partially crystallized and the O-rich sub-layers are completely amorphous (Fig. 2.c and d). Moreover, the systematic HRTEM study reveals that the crystallization starts for $\lambda_{met} > 10$ nm with small crystallite size (3 to 5 nm) and finishes with a